Original Article

Innate Immunity

Innate Immunity
2022, Vol. 28(1): 37–48

DOI: 10.1177/17534259211069104
journals.sagepub.com/home/ini
SAGE

Circ_0026579 alleviates LPS-induced WI-38 cells inflammation injury in infantile pneumonia

Yang Yu[1], Tingting Yang[1], Zhaozheng Ding[2] and Yuan Cao[2]

Abstract

Circular RNA (circRNA) represents an important regulator in infantile pneumonia progression. To clarify the role of circ_0026579 in this disease, LPS was used to treat WI-38 cells to mimic inflammation injury. The levels of inflammatory factors were determined by ELISA assay. Cell proliferation and apoptosis were measured by MTT assay, EdU staining and flow cytometry. The protein levels of cyclinD1, cleaved-caspase-3 and insulin-like growth factor 2 (IGF2) were examined using Western blot analysis. Cell oxidative stress was assessed by detecting MDA level and SOD activity. The expression of circ_0026579, miR-24-3p and IGF2 were analyzed using quantitative real-time PCR, and the interaction between miR-24-3p and circ_0026579 or IGF2 was confirmed by dual-luciferase reporter assay and RIP assay. LPS induced inflammation in WI-38 cells. Circ_0026579 expression was promoted in LPS-induced WI-38 cells, and its knockdown alleviated LPS-induced WI-38 cells inflammation. MiR-24-3p was sponged by circ_0026579, and its expression was reduced by LPS. MiR-24-3p inhibitor reversed the regulation of circ_0026579 knockdown on LPS-induced WI-38 cells inflammation. IGF2 was targeted by miR-24-3p, and its expression could be enhanced by LPS. MiR-24-3p relieved the inflammation of WI-38 cells which could be abolished by IGF2 overexpression. Circ_0026579 positively regulated IGF2 expression through sponging miR-24-3p. Circ_0026579 knockdown alleviated LPS-induced WI-38 cells inflammation by miR-24-3p/IGF2 axis, suggesting that circ_0026579 might contribute to infantile pneumonia progression.

Keywords

Infantile pneumonia, circ_0026579, miR-24-3p, IGF2

Date received: 30 September 2021; revised: 1 December 2021; accepted: 8 December 2021

Introduction

Infantile pneumonia is a common respiratory disease in young children and infants, and it can cause heart failure and other complications in severe cases.[1] At present, most of the treatment methods for infantile pneumonia are antiviral and antibacterial treatment, but with the increase of the use of antibiotics, the increase of pathogen resistance makes the disease difficult to cure.[2] Therefore, in-depth research on the pathogenesis of infantile pneumonia and finding more effective targets is of great significance for the treatment of infantile pneumonia. LPS is a Gram-negative bacterial endotoxin, which plays a key role in the inflammatory response associated with infantile pneumonia.[3,4] Studies have found that LPS can cause high expression of chemokines and inflammatory factors in a variety of cells both *in vivo* and *in vitro*, so it is often used to induce cellular inflammatory models in many diseases, including infantile pneumonia.[5,6]

Circular RNA (circRNA), a non-coding RNA with a special circular structure, is highly conserved and stable in organisms.[7] Functionally, most circRNAs have been confirmed to contain microRNA (miRNA) response elements, which can regulate target genes expression by interacting with miRNAs.[8] In recent years, circRNA has been proved to be a key regulator for the progression of many human diseases.[9] Currently, many studies have confirmed that circRNA plays an important role in LPS-induced lung cells inflammation injury. For example, circVMA21 overexpression could alleviate LPS-triggered inflammation injury in WI-38 cells by interacting miR-142-3p,[10] while

[1]Department of Neonatology, The First People's Hospital of Lianyungang, Lianyungang, Jiangsu, China
[2]Department of Paediatric surgery, The First People's Hospital of Lianyungang, Lianyungang, Jiangsu, China

Corresponding author:
Yuan Cao, Department of Paediatric surgery, The First People's Hospital of Lianyungang, No.182, Tongguan North Road, Haizhou District, Lianyungang, 222000, China.
Email: Lygyy4010@163.com

circZNF652 knockdown could relieve the inflammation injury in LPS-induced WI-38 cells through sponging miR-181a.[11] Therefore, circRNA is an important molecule regulating infantile pneumonia progression and is expected to become a potential molecular target for infantile pneumonia therapy.

In a past study, Zhao et al. used microarray analysis and found that circ_0026579 (derived from ESPL1 gene) was significantly highly expressed in the blood of patients with community-acquired pneumonia.[12] We speculated that circ_0026579 might be a possible potential target for pneumonia. Unfortunately, the role of circ_0026579 in infantile pneumonia is unclear. Our study aims to clarify the function and potential molecular mechanism of circ_0026579 in infantile pneumonia using LPS-induced WI-38 cells inflammation injury, and to use the hypothesis of circRNA/miRNA/mRNA axis to reveal its potential molecular mechanism.

Materials and methods

Cell culture and LPS treatment

Human embryonic lung fibroblast cells (WI-38) were bought from ATCC (Rockville, MD, USA) and cultured in EMEM medium (ATCC) containing 10% FBS (Gibco, Carlsbad, CA, USA) and 1% penicillin-streptomycin (Invitrogen, Carlsbad, CA, USA) at 37°C with 5% CO_2. Different concentrations (0, 5, 10, and 15 μg/ml) of LPS (from *Escherichia coli 055:B5*, Solarbio, Beijing, China) was used to treat cells for 12 h to screen the optimum treatment concentration.

ELISA assay

According to the instructions of Human IL-6 and TNF-α ELISA Kits (Sigma-Aldrich, St Louis, MO, USA), the concentrations of IL-6 and TNF-α in the culture supernatant of WI-38 cells were determined.

Table 1. Primer sequences used for qRT-PCR.

Name	Primer sequences (5'-3')
circ_0026579	F: AAGTGATTTTCCCCAGTGTTTT
	R: CTCCTCTCAGCATCAGATCG
ESPL1	F: CCGCCTTGAAGGAGTTCCTG
	R: GGGGTAGACACTAAGTAGCCAT
miR-24-3p	F: GCCGAGTGGCTCAGTTCAGCAG
	R: CAGTGCGTGTCGTGGAGT
IGF2	F: GTGGCATCGTTGAGGAGTG
	R: CACGTCCCTCTCGGACTTG
U6	F: ATTGGAACGATACAGAGAAGATT
	R: GGAACGCTTCACGAATTTG
GAPDH	F: CAATGACCCCTTCATTGACC
	R: TGGAAGATGGTGATGGGATT

Cell proliferation assay

WI-38 cells were plated into 96-well plates (5×10^3 cells/well for MTT assay; 1×10^5 cells/well for EdU staining) and cultured for 48 h. Based on the instructions of MTT Assay Kit (Abcam, Cambridge, MA, USA), the absorbance at 590 nm was determined by a microplate reader to examine cell viability. EdU staining was performed according to the instructions of BeyoClick™ EdU Cell Proliferation Kit (Beyotime). Cell nucleus was stained by DAPI solution (Beyotime). EdU positive cell rate was calculated by ImageJ software.

Cell apoptosis assay

Cell apoptosis was evaluated by Annexin V-FITC Apoptosis Detection Kit (Solarbio). In brief, WI-38 cells (5×10^5 cells) were re-suspended with binding buffer. After stained by Annexin V-FITC and propidium iodide, cell apoptosis rate was analyzed by flow cytometer.

Western blot (WB) analysis

RIPA lysis buffer (Beyotime) was applied for extracting total protein. Protein was subjected to SDS-PAGE gel and transferred to PVDF membranes. The membranes were incubated with primary Ab and secondary Ab. The protein blots were visualized by an enhanced chemiluminescence reagent (Solarbio). All Abs were bought from Abcam. The primary Ab included anti-cyclinD1 (1:5,000, ab226977), anti-cleaved-caspase-3 (1:500, ab2302), anti-IGF2 (1:10,000, ab9574) and anti-GAPDH (1:2,500, ab9485). The secondary Ab was goat anti-rabbit IgG (1:50,000, ab205718).

Determine of cell oxidative stress

MDA level and SOD activity were determined to assess cell oxidative stress. The supernatant of WI-38 cells were collected for detecting MDA level and SOD activity using the MDA Assay Kit and SOD Activity Assay Kit (all from Solarbio) according to the kit instructions.

Quantitative real-time PCR (qRT-PCR)

The isolation of total RNA was performed using TRIzol reagent (Invitrogen). The cDNA was synthesized using Primescript RT Reagent Kit (Takara, Tokyo, Japan). After that, qRT-PCR was carried out on PCR instrument with SYBR Premix Ex Taq™ Reagent (Takara). The $2^{-\Delta\Delta Ct}$ method was used to analyze relative expression with GAPDH or U6 as endogenous control. Primer sequences were shown in Table 1.

Identification of circRNA

In subcellular localization analysis, the nucleus and cytoplasm RNA of WI-38 cells were separately isolated by PARIS Kit (Invitrogen). Using U6 as nucleus control and GAPDH as cytoplasm control, qRT-PCR was utilized for measuring circ_0026579 expression. In RNase R assay, the RNA from WI-38 cells was incubated with RNase R (Geneseed, Guangzhou, China). The circ_0026579 expression and linear ESPL1 mRNA expression were examined by qRT-PCR.

Cell transfection

The circ_0026579 small interference RNA and pCD5 overexpression vector (si-circ_0026579 and circ_0026579), miR-24-3p mimic or inhibitor (miR-24-3p or anti-miR-24-3p), and pcDNA insulin-like growth factor 2 (IGF2) overexpression vector, as well as their matched negative controls were synthesized by RiboBio (Guangzhou, China). Cell transfection was carried out using Lipofectamine 3000 (Invitrogen). After transfection for 24 h, the cells were treated with 10 μg/ml LPS for 12 h.

Dual-luciferase reporter assay

This assay was performed using Dual-Luciferase Reporter Assay Kit (Vazyme, Nanjing, China). In brief, the wild type (WT) or mutant type (MUT) vectors for circ_0026579 or IGF2 3'UTR were constructed using the psiCHECK2 reporter vector. 293 T cells were transfected with the above vectors and miR-24-3p mimic or miR-NC. Following 24 h of cell incubation, relative luciferase activity was calculated by detecting the luciferase activity ratio of *Firefly* to *Renilla*.

RIP assay

Ago2 is the core component of RNA-induced silencing complex and is the key to the function of miRNA. Under appropriate conditions, the immuno-purification of Ago2 can be performed to confirm the interaction between miRNA and target genes by detecting the enrichment of miRNA and target genes. IgG does not specifically bind to any RNA or protein, so IgG was used as a negative control. Briefly, WI-38 cells were lysed with RIP lysis buffer (Millipore, Darmstadt, Germany), and then cell lysates were incubated with magnetic beads (Millipore) conjugated with anti-IgG or anti-Ago2 at 4°C overnight. QRT-PCR was used to determine RNA expression in the immuno-precipitated RNA.

Statistical analysis

Data were displayed as mean ± SD from at least 3 independent experiments. GraphPad Prism 8.0 software was used for data analysis. Student's *t*-test or one-way ANOVA followed by Tukey post hoc test was conducted for comparison. $P < 0.05$ was regarded as statistically significant.

Results

LPS stimulation induced inflammation injury in WI-38 cells

To screen for the optimal treatment concentration of LPS, we evaluated WI-38 cell function at different concentrations of LPS. Our data showed that the concentrations of inflammatory factors IL-6 and TNF-α in WI-38 cells were markedly increased with the increase of LPS concentration (Figure 1A). Also, the viability and EdU positive cells were significantly decreased with the increase of LPS concentration (Figure 1B-C). By detecting apoptosis rate, we discovered that the apoptosis of WI-38 cells was increased significantly in a concentration-dependent manner under different concentrations of LPS (Figure 1D). CyclinD1 is listed as proliferation-related factor, while cleaved-casp-3 is listed as apoptosis-associated markers. Here, we measured the protein levels of CyclinD1 and cleaved-caspase-3. The results showed that CyclinD1 protein level was gradually reduced while cleaved-caspase-3 protein level was gradually enhanced with the increase of LPS concentration (Figure 1E). Under the treatment of LPS, the MDA level was promoted, and SOD activity was inhibited in a concentration-dependent manner (Figure 1F-G). These data revealed that LPS could induce inflammation injury in WI-38 cells. After evaluation, we chose 10 μg/ml LPS for functional test

Circ_0026579 expression was increased in LPS-stimulated WI-38 cells

In different concentrations of LPS treatment, the expression of circ_0026579 was increased gradually in a concentration-dependent manner (Figure 2A). To evaluate the circular characteristics of circ_0026579, subcellular localization analysis and RNase R assay were performed. The results showed that circ_0026579 was mainly present in the cytoplasm and could resist the digestion of RNase R compared with linear RNA ESPL1 (Figure 2B-C). These results confirmed that circ_0026579 indeed had a circular structure.

Knockdown of circ_0026579 alleviated cell inflammation injury

To determine the role of circ_0026579 in lung cell inflammation injury, WI-38 cells were transfected with si-circ_0026579 and then treated with 10 μg/ml LPS. The increased circ_0026579 expression regulated by LPS could be reduced by si-circ_0026579 (Figure 3A). The

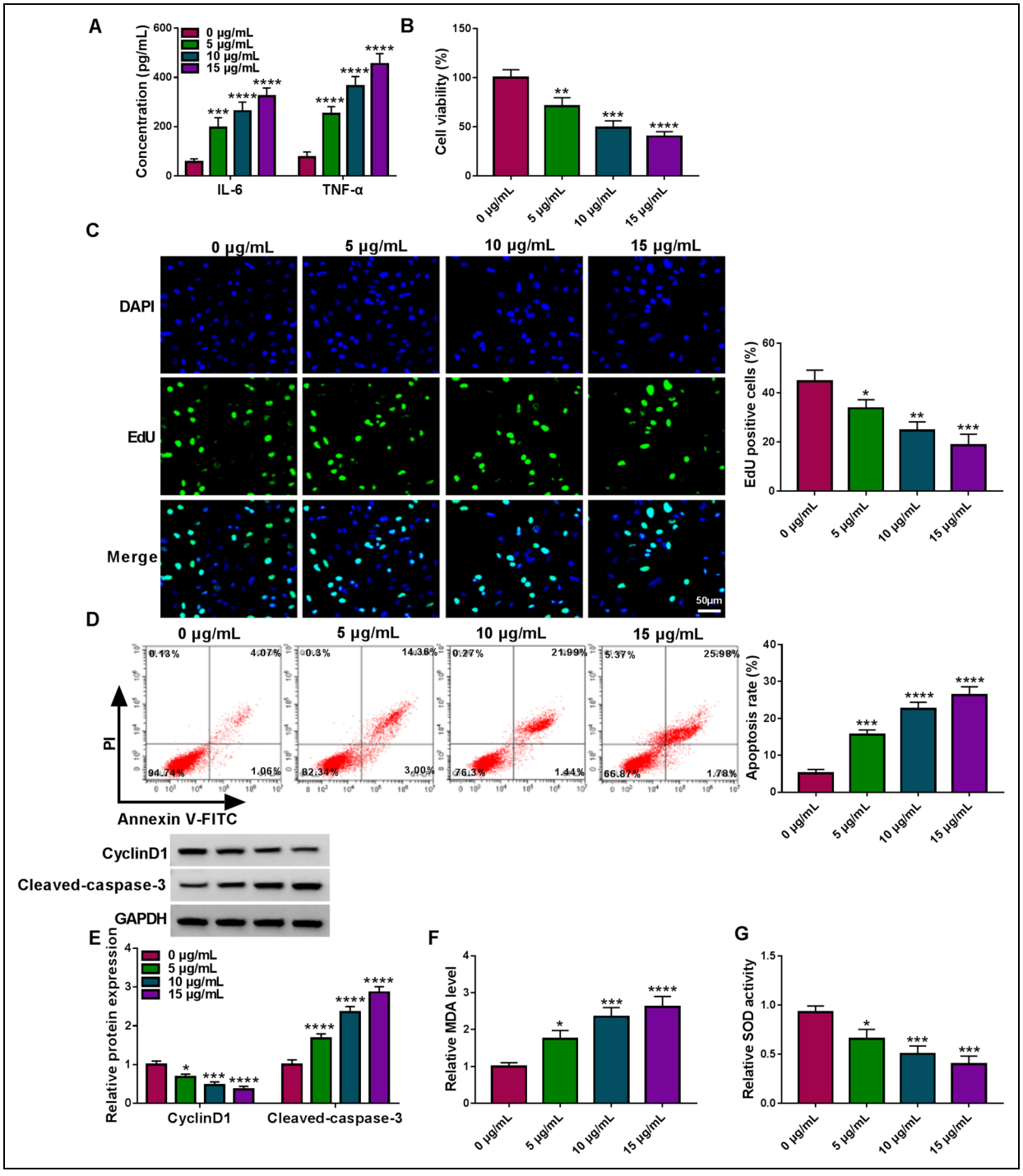

Figure 1. LPS stimulation induced inflammation injury in WI-38 cells. WI-38 cells were treated with different concentrations of LPS. (A) The concentrations of IL-6 and TNF-α were determined by ELISA assay. MTT assay (B), EdU staining (C) and flow cytometry (D) were used to measure cell proliferation and apoptosis. (E) The protein levels of cyclinD1 and cleaved-caspase-3 were detected by WB analysis. (F-G) The MDA level and SOD activity were assessed using corresponding Assay Kits. *$P < 0.05$, **$P < 0.01$, ***$P < 0.001$, ****$P < 0.0001$.

promotion effect of LPS on the concentrations of IL-6 and TNF-α in WI-38 cells could be abolished by circ_0026579 silencing (Figure 3B). Moreover, silenced circ_0026579 remarkably enhanced the viability and EdU positive cells and reduced the apoptosis rate in LPS-induced WI-38 cells (Figure 3C-E). Besides, circ_0026579 knockdown

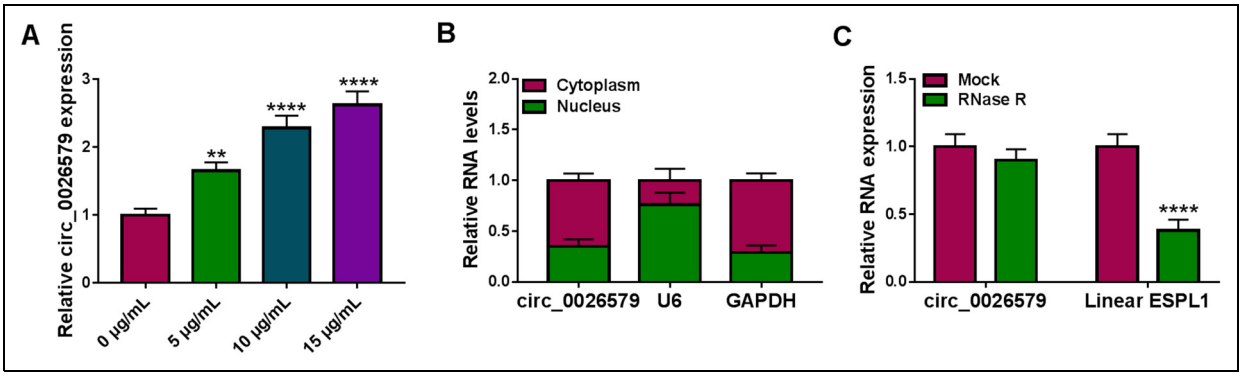

Figure 2. Circ_0026579 expression was increased in LPS-stimulated WI-38 cells. (A) The expression of circ_0026579 was measured by qRT-PCR in WI-38 cells treated with different concentrations of LPS. Subcellular localization analysis (B) and RNase R (C) were used to assess the circular characteristics of circ_0026579. $^{**}P < 0.01$, $^{****}P < 0.0001$.

also increased cyclinD1 protein expression, while decreased cleaved-caspase-3 protein expression in LPS-induced WI-38 cells (Figure 3F). Furthermore, silencing of circ_0026579 inhibited the oxidative stress in WI-38 cells enhanced by LPS, which was manifested by the decreased MDA level and increased SOD activity (Figure 3G-H). Therefore, we confirmed that circ_0026579 might promote the progression of infantile pneumonia.

Circ_0026579 directly interacted with miR-24-3p

To search for the targeted miRNA for circ_0026579, the starBase v2.0 software was used. In the previous study, 7 miRNAs related to lung injury or pneumonia were selected as candidate miRNAs according to the prediction results of starBase v2.0 software. By detecting the expression of each miRNA after circ_0026579 knockdown, we determined that circ_0026579 had the most significant promotion effect on miR-24-3p expression (Supplemental Figure 1A), so miR-24-3p was selected as the target of circ_0026579 for study. The binding sites between circ_0026579 and miR-24-3p are shown in Figure 4A. Dual-luciferase reporter assay and RIP assay were performed to assess the interaction between circ_0026579 and miR-24-3p. The results confirmed that miR-24-3p mimic could inhibit the luciferase activity of WT-circ_0026579 vector without affecting that of the MUT-circ_0026579 vector (Figure 4B), and both miR-24-3p and circ_0026579 could significantly enrich in Ago2 (Figure 4C). In addition, we found that LPS could inhibit miR-24-3p expression, and miR-24-3p expression was decreased significantly with the increase of LPS concentration (Figure 4D). In addition, we confirmed that pCD5 circ_0026579 overexpression vector markedly enhanced circ_0026579 expression in LPS-induced WI-38 cells (Figure 4E). Through detecting miR-24-3p expression, we found that miR-24-3p expression could be promoted by circ_0026579 silencing, while suppressed by circ_0026579 overexpression in LPS-induced WI-38 cells (Figure 4F).

MiR-24-3p inhibitor reversed the suppressive effect of circ_0026579 silencing on cell inflammation injury

The detection results of miR-24-3p expression suggested that anti-miR-24-3p indeed reduced miR-24-3p expression in WI-38 cells (Figure 5A). Then, WI-38 cells were co-transfected with si-circ_0026579 and anti-miR-24-3p followed by treatment with LPS to explore whether miR-24-3p participated in the regulation of circ_0026579 on infantile pneumonia progression. The addition of anti-miR-24-3p reversed the increasing effect of si-circ_0026579 on miR-24-3p expression in LPS-induced WI-38 cells (Figure 5B). The inhibition effect of circ_0026579 knockdown on the concentrations of IL-6 and TNF-α in LPS-induced WI-38 cells could be reversed by miR-24-3p inhibitor (Figure 5C). The enhancing effect of circ_0026579 knockdown on the viability, the EdU positive cells and cyclinD1 protein expression, as well as the repressing on the apoptosis rate and cleaved-caspase-3 protein expression in LPS-induced WI-38 cells also could be abolished by the addition of anti-miR-24-3p (Figure 5D-H). Moreover, miR-24-3p inhibitor overturned the decreasing effect of circ_0026579 silencing on MDA level and the increasing effect on SOD activity in LPS-induced WI-38 cells (Figure 5I-J). These data verified that circ_0026579 sponged miR-24-3p to regulate the progression of infantile pneumonia.

MiR-24-3p targeted IGF2

The starBase v2.0 software also was used to predict the target of miR-24-3p, and 7 targets related to lung injury or pneumonia were selected as candidate targets for miR-24-3p. After overexpressing miR-24-3p, we

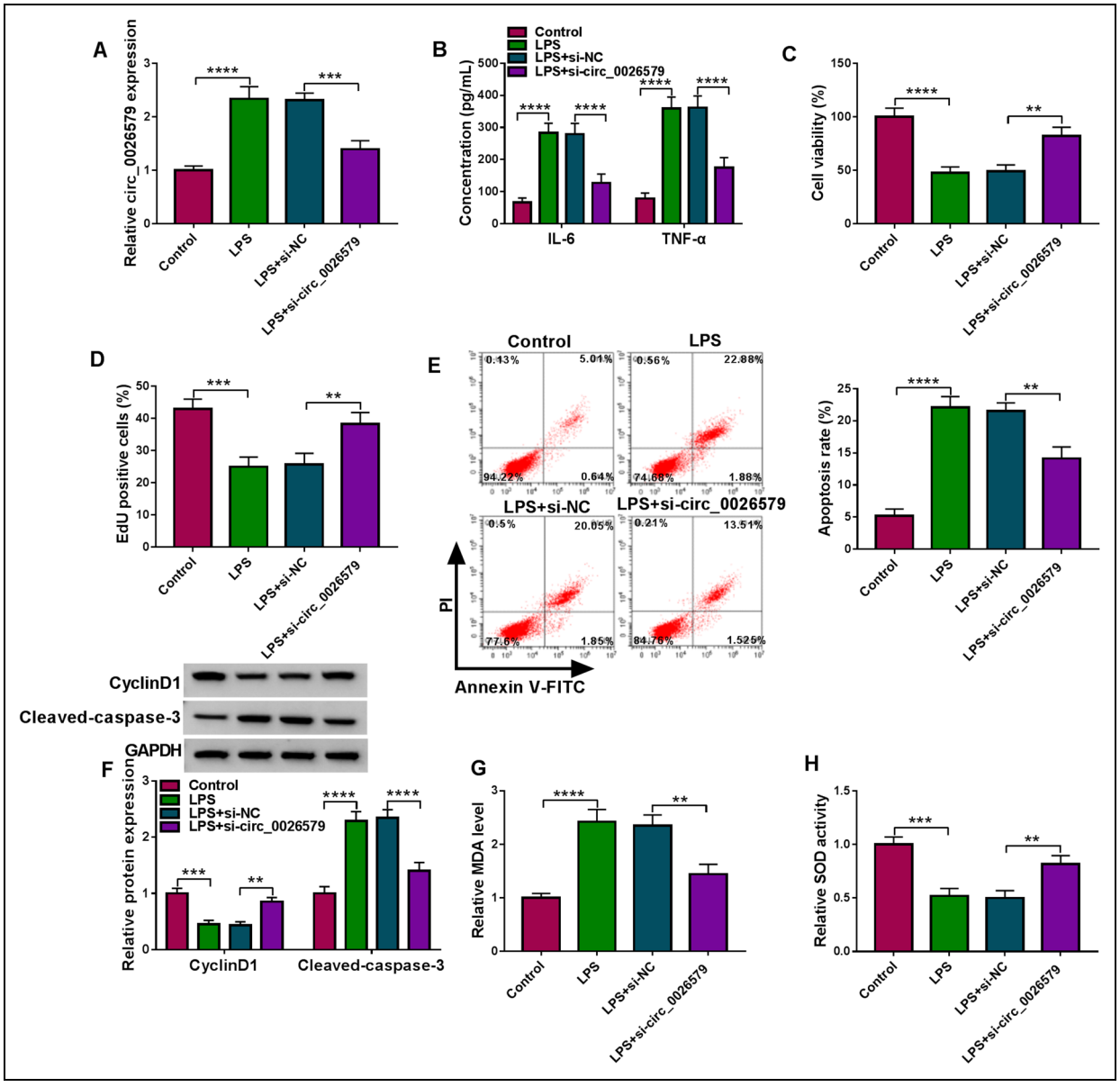

Figure 3. Effects of circ_0026579 knockdown on cell inflammation injury. WI-38 cells were transfected with si-NC or si-circ_0026579 followed by treatment with 10 μg/ml LPS. (A) The circ_0026579 expression was detected by qRT-PCR. (B) ELISA was used to measure the concentrations of IL-6 and TNF-α. Cell proliferation and apoptosis were determined using MTT assay (C), EdU staining (D) and flow cytometry (E). (F) WB analysis was performed to examine the protein levels of cyclinD1 and cleaved-caspase-3. (G-H) Corresponding Assay Kits were used to evaluate the MDA level and SOD activity. $^{**}P < 0.01$, $^{***}P < 0.001$, $^{****}P < 0.0001$.

discovered that miR-24-3p had the most significant inhibition effect on IGF2 expression (Supplemental Figure 1B), so IGF2 was selected as the target of miR-24-3p for study. The binding sites between miR-24-3p and IGF2 3'UTR are shown in Figure 6A. Further analysis confirmed that miR-24-3p mimic only could reduce the luciferase activity of WT-IGF2 3'UTR vector (Figure 6B), and both miR-24-3p and IGF2 also could be markedly enriched in Ago2 (Figure 6C). These data confirmed the interaction between miR-24-3p and IGF2. With the increase of LPS concentration, we found that IGF2 protein expression was gradually increased in WI-38 cells (Figure 6D). After determined that miR-24-3p expression could be promoted by miR-24-3p mimic and inhibited by miR-243-3p inhibitor (Figure 6E), we discovered that IGF2 expression was decreased by miR-24-3p overexpression, while increased by miR-24-3p inhibition (Figure 6F). All data illuminated that IGF2 was a target of miR-24-3p.

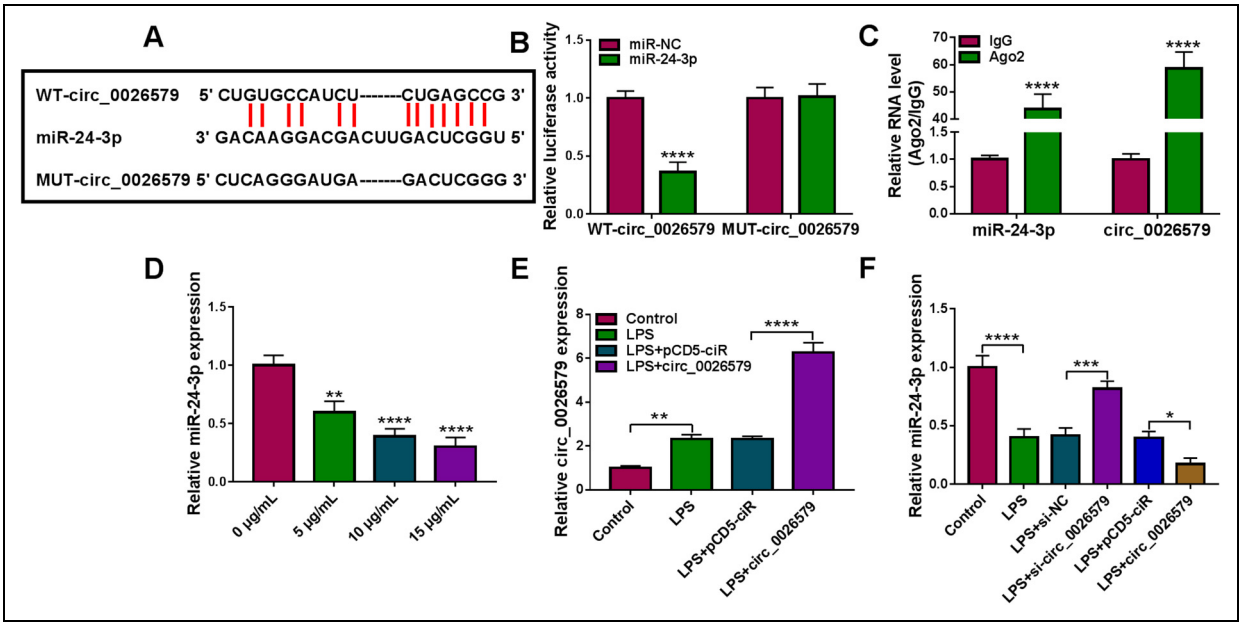

Figure 4. Circ_0026579 interacted with miR-24-3p. (A) The sequences of WT/MUT-circ_0026579 are shown. Dual-luciferase reporter assay (B) and RIP assay (C) were used to assess the interaction between circ_0026579 and miR-24-3p. (D) QRT-PCR was performed to measure miR-24-3p expression in WI-38 cells treated with different concentrations of LPS. (E) The circ_0026579 expression was detected by qRT-PCR in LPS-induced WI-38 cells transfected with pCD5 circ_0026579 overexpression vector. (F) MiR-24-3p expression was determined by qRT-PCR in LPS-induced WI-38 cells transfected with si-circ_0026579 or pCD5 circ_0026579 overexpression vector. *$P < 0.05$, **$P < 0.01$, ***$P < 0.001$, ****$P < 0.0001$.

MiR-24-3p inhibited cell inflammation injury by targeting IGF2

The pcDNA IGF2 overexpression vector was transfected into WI-38 cells and the increased IGF2 expression confirmed its transfection efficiency (Figure 7A). Subsequently, WI-38 cells were co-transfected with miR-24-3p mimic and pcDNA IGF2 overexpression vector followed by treatment with LPS to perform the rescue experiments. The addition of pcDNA IGF2 overexpression vector could abolish the decreasing effect of miR-24-3p mimic on IGF2 protein expression in LPS-induced WI-38 cells (Figure 7B). The suppressive effect of miR-24-3p on the concentrations of IL-6 and TNF-α in LPS-induced WI-38 cells could be overturned by IGF2 overexpression (Figure 7C). Also, miR-24-3p promoted the viability, increased the EdU positive cells and repressed the apoptosis rate of LPS-induced WI-38 cells, while these effects could be reversed by overexpressing IGF2 (Figure 7D-G). Meanwhile, IGF2 overexpression also reversed the increasing effect of miR-24-3p on cyclinD1 protein expression and the decreasing effect on cleaved-caspase-3 protein expression (Figure 7H). In addition, miR-24-3p reduced MDA level and enhanced SOD activity in LPS-induced WI-38 cells, and overexpressed IGF2 also could abolish these effects (Figure 7I-J). Hence, our data suggested that miR-24-3p targeted IGF2 to inhibit the progression of infantile pneumonia.

Circ_0026579 positively regulated IGF2 by sponging miR-24-3p

The above results pointed out that circ_0026579 could sponge miR-24-3p and miR-24-3p could target IGF2. To explore whether circ_0026579 regulated IGF2 expression by sponging miR-24-3p, we detected IGF2 expression in LPS-induced WI-38 cells transfected with si-circ_0026579 and anti-miR-24-3p. Our data showed that circ_0026579 knockdown could inhibit the mRNA and protein expression of IGF2, while these effects could be reversed by miR-24-3p inhibitor (Figure 8A-B).

Discussion

Infantile pneumonia has become one of the leading causes of death among children in the world.[13] It is imperative to elucidate the mechanisms that affect the inflammation injury of lung cells and reveal the potential molecular targets for the treatment of infantile pneumonia. Therefore, we treated WI-38 cells with LPS to construct an *in vitro* inflammation injury model of lung cells. Our data confirmed that the induction of LPS could lead to inflammation, apoptosis and oxidative stress in WI-38 cells, which confirmed the success of the *in vitro* model. We noted that circ_0026579 expression was significantly up-regulated in LPS-treated WI-38 cells. Circ_0026579 knockdown had an inhibitory effect on LPS-induced cell

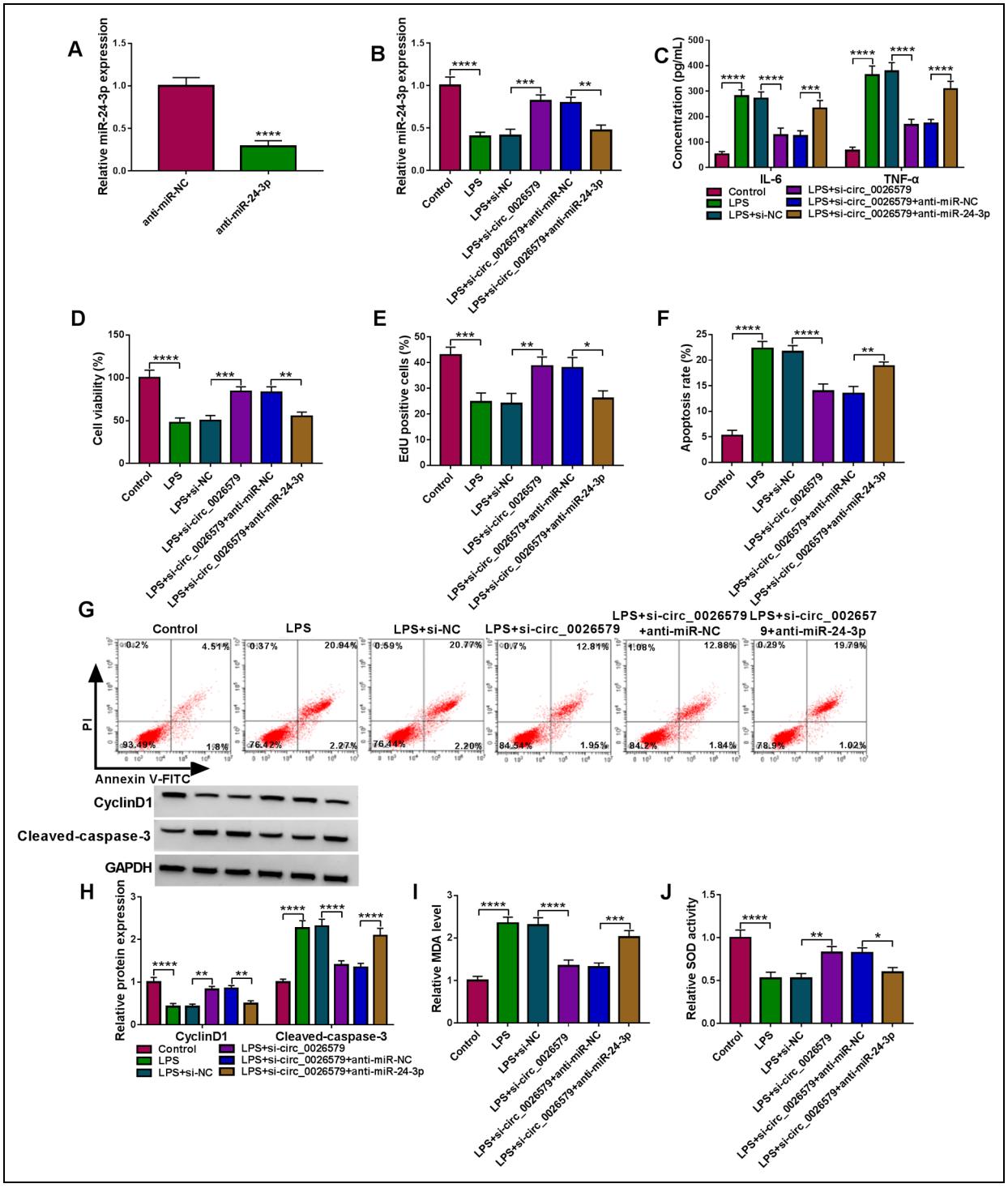

Figure 5. Effects of circ_0026579 silencing and miR-24-3p inhibitor on cell inflammation. (A) The miR-24-3p expression was measured by qRT-PCR. (B-J) WI-38 cells were co-transfected with si-circ_0026579 and anti-miR-24-3p followed by treatment with LPS. (B) QRT-PCR was used to detect miR-24-3p expression. (C) The concentrations of IL-6 and TNF-α were assessed using ELISA assay. MTT assay (D), EdU staining (E) and flow cytometry (F-G) were performed to evaluate cell proliferation and apoptosis. (H) WB analysis was utilized for testing the protein levels of cyclinD1 and cleaved-caspase-3. (I-J) The MDA level and SOD activity were analyzed by corresponding Assay Kits. *$P < 0.05$, **$P < 0.01$, ***$P < 0.001$, ****$P < 0.0001$.

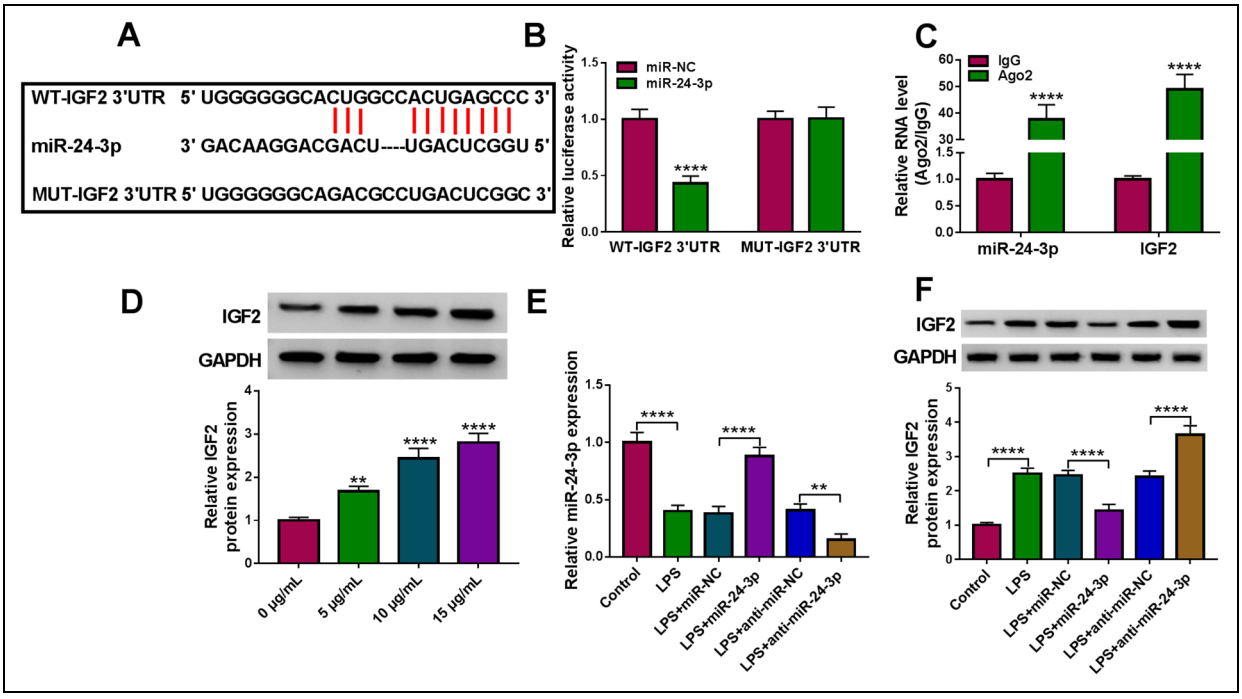

Figure 6. MiR-24-3p targeted IGF2. (A) The sequences of WT/MUT-IGF2 3'UTR were exhibited. The interaction between IGF2 and miR-24-3p was confirmed using dual-luciferase reporter assay (B) and RIP assay (C). (D) WB analysis was used to examine IGF2 protein expression in WI-38 cells treated with different concentrations of LPS. (E) The miR-24-3p expression was measured by qRT-PCR in LPS-induced WI-38 cells transfected with miR-24-3p mimic or inhibitor. (F) IGF2 protein expression was assessed by WB analysis in LPS-induced WI-38 cells transfected with miR-24-3p mimic or inhibitor. $^{**}P < 0.01$, $^{****}P < 0.0001$.

inflammation injury. This was a surprising finding, suggesting that circ_0026579 knockdown might be an effective treatment strategy for infantile pneumonia.

The idea that circRNAs act as miRNA sponges to regulate target expression has been confirmed in many studies.[14,15] Here, we proposed that circ_0026579 could act as a ceRNA for miR-24-3p. In past studies, miR-24-3p has been shown to possess an important role in the malignant progression of lung cancer and pulmonary related disease. Yan et al. reported that miR-24-3p could aggravate lung cancer progression by enhancing cancer cell proliferation and migration.[16] According to a recent study, miR-24-3p was discovered to inhibit DNA damage response and apoptosis of lung epithelial cells, which might be a biomarker for treating chronic obstructive pulmonary disease.[17] In acute lung injury, miR-24 had been found to inhibit LPS-induced inflammation injury in neonatal rats.[18] Consistent with these data, our data showed that miR-24-3p inhibited the inflammation injury in LPS-induced WI-38 cells, confirming the anti-inflammatory role of miR-24-3p. Besides, miR-24-3p inhibitor abolished the negative regulation of circ_0026579 knockdown on LPS-induced cell inflammation injury, which suggested that circ_0026579 indeed targeted miR-24-3p to mediate inflammation injury.

IGF2 is the first discovered endogenous imprinted gene, which plays a vital function in cell differentiation, proliferation and embryo development.[19,20] A large number of studies have shown that IGF2 is highly expressed in many cancers, and it can work as an oncogene to promote their malignant progression, including ovarian,[21] colorectal[22] and breast cancer.[23] In pneumonia-related studies, Zhang et al. showed that IGF2 contributed to LPS-induced inflammation injury, confirming that it might aggravate acute pneumonia.[24] Importantly, knockdown of IGF2 was considered to inhibit the production of inflammatory factors to alleviate LPS-induced cell injury in acute pneumonia.[25] Here, we confirmed that LPS could induce IGF2 expression in WI-38 cells, and its overexpression abolished the inhibitory effect of miR-24-3p on LPS-induced cell inflammation injury. These data revealed that miR-24-3p relieved inflammation injury by targeting IGF2. Furthermore, our data also verified that circ_0026579 positively regulated IGF2 via targeting miR-24-3p. Above all, the circ_0026579/miR-24-3p/IGF2 network was confirmed in this research.

In summary, our study pointed out a novel circRNA that regulated infantile pneumonia progression. This study showed that circ_0026579 knockdown alleviated LPS-induced WI-38 cells inflammation injury, mainly through the regulation of miR-24-3p/IGF2 axis. The

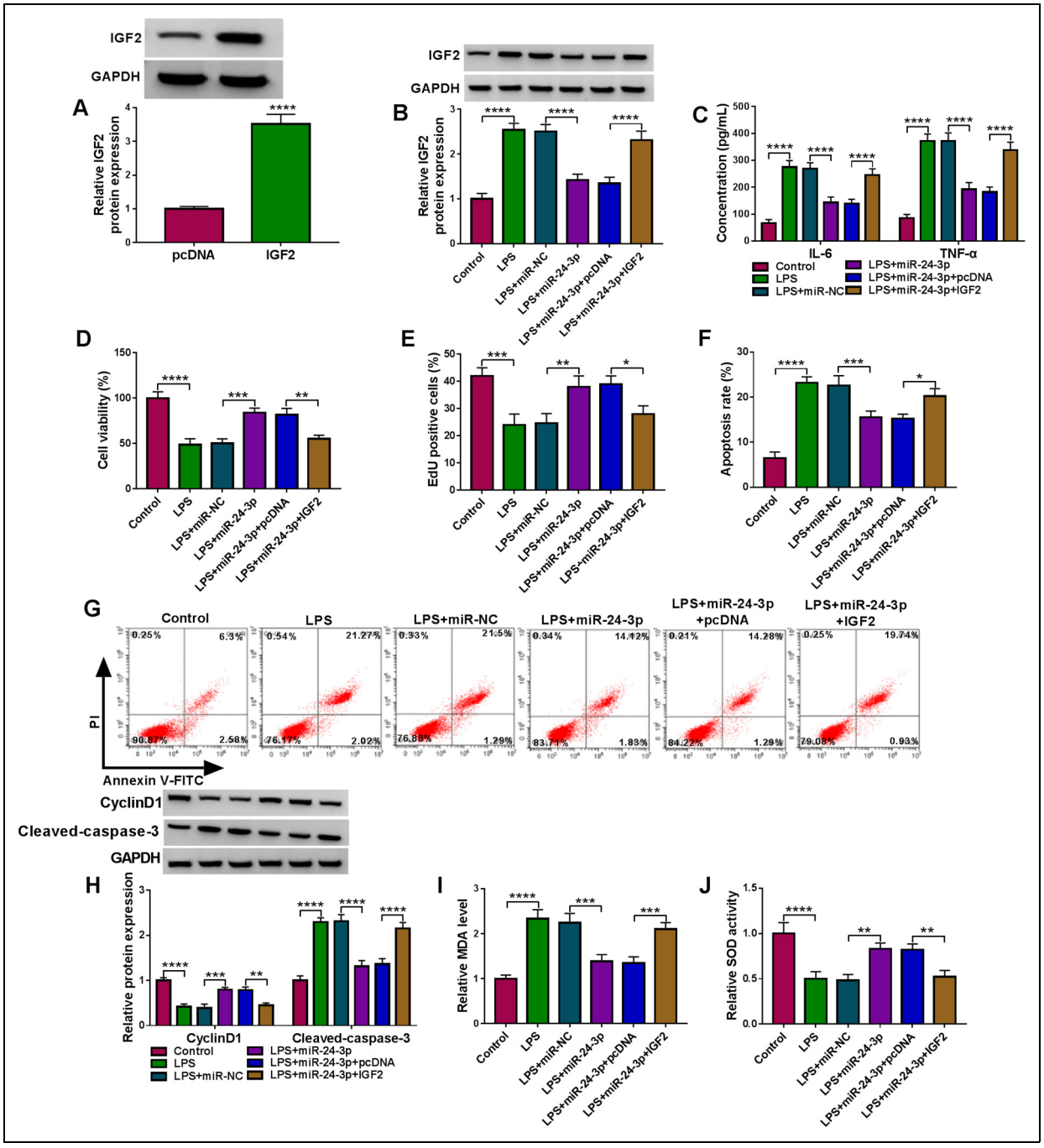

Figure 7. MiR-24-3p inhibited cell inflammation injury by targeting IGF2. (A) The IGF2 protein expression was examined by WB analysis. (B-J) WI-38 cells were co-transfected with miR-24-3p and IGF2 followed by treated with LPS. (B) WB analysis was used to measure IGF2 protein expression. (C) ELISA assay was performed to examine the concentrations of IL-6 and TNF-α. Cell proliferation and apoptosis were analyzed using MTT assay (D), EdU staining (E) and flow cytometry (F-G). (H) The protein levels of cyclinD1 and cleaved-caspase-3 were measured using WB analysis. (I-J) Corresponding Assay Kits were used to determine the MDA level and SOD activity. *$P < 0.05$, **$P < 0.01$, ***$P < 0.001$, ****$P < 0.0001$.

results of this study might provide a new direction for clinical treatment of infantile pneumonia. Still, the current study has some limitations. We have not yet established a mouse model for *in vivo* experiments. In future studies, we will conduct *in vivo* assay to further confirm our conclusions.

Ethics approval and consent to participate

The present study was approved by the ethical review committee of The First People's Hospital of Lianyungang. Written informed consent was obtained from all enrolled patients.

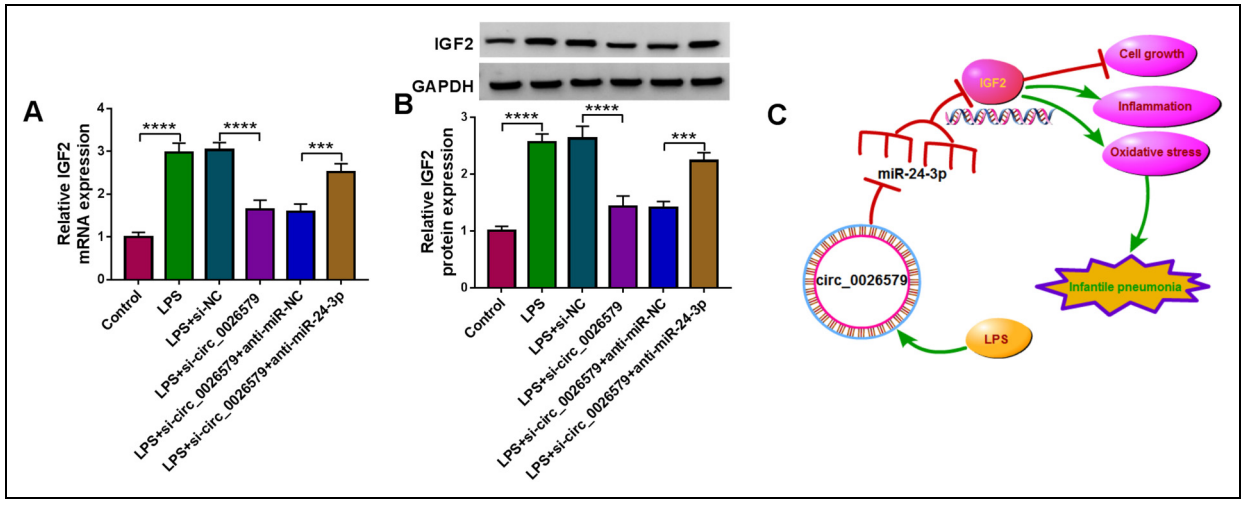

Figure 8. Circ_0026579 positively regulated IGF2 by sponging miR-24-3p. (A-B) WI-38 cells were co-transfected with si-circ_0026579 and anti-miR-24-3p followed by treated with LPS. The mRNA and protein expression levels of IGF2 were determined using qRT-PCR and WB analysis. (C) The main idea diagram of this study. ***$P < 0.001$, ****$P < 0.0001$.

Consent for publication

Patients agree to participate in this work.

Availability of data and materials

The analyzed data sets generated during the present study are available from the corresponding author on reasonable request

Competing interests

The authors declare that they have no competing interests.

Declaration of conflicting interests

The author(s) declared no potential conflicts of interest with respect to the research, authorship, and/or publication of this article.

Funding

The author(s) received no financial support for the research, authorship and/or publication of this article.

ORCID iD

Yuan Cao https://orcid.org/0000-0002-2694-622X

Supplemental material

Supplemental material for this article is available online.

References

1. Zhang J, Wang CH, Liu XJ, et al. Efficacy and safety analysis of dopamine combined with creatine phosphate sodium in the treatment of infantile pneumonia combined with heart failure. *J Biol Regul Homeost Agents* Nov-Dec 2020; 34: 2103–2108.
2. Cohen R, Angoulvant F, Biscardi S, et al. Antibiotic treatment of lower respiratory tract infections. *Archives de pediatrie : organe officiel de la Societe francaise de pediatrie* Dec 2017; 24: S17–S21.
3. Bai D, Han A and Cong S. The effect of down-regulation of CCL5 on lipopolysaccharide-induced WI-38 fibroblast injury: a potential role for infantile pneumonia. *Iran J Basic Med Sci* May 2018; 21: 449–454.
4. Liu Q, Yang H, Xu S, et al. Downregulation of p300 alleviates LPS-induced inflammatory injuries through regulation of RhoA/ROCK/NF-kappaB pathways in A549 cells. *Biomedicine & pharmacotherapy = Biomedecine & pharmacotherapie* Jan 2018; 97: 369–374.
5. Bai D, Cong S and Zhu LP. Attenuation of focal adhesion kinase reduces lipopolysaccharide-induced inflammation injury through inactivation of the Wnt and NF-kappaB pathways in A549 cells. *Biochemistry Mosc* Apr 2017; 82: 446–453.
6. Quan B, Zhang H and Xue R. miR-141 alleviates LPS-induced inflammation injury in WI-38 fibroblasts by up-regulation of NOX2. *Life Sci* Jan 1 2019; 216: 271–278.
7. Chen LL and Yang L. Regulation of circRNA biogenesis. *RNA Biol* 2015; 12: 381–388.
8. Xiao Y. Construction of a circRNA-miRNA-mRNA network to explore the pathogenesis and treatment of pancreatic ductal adenocarcinoma. *J Cell Biochem* Jan 2020; 121: 394–406.
9. Kristensen LS, Andersen MS, Stagsted LVW, et al. The biogenesis, biology and characterization of circular RNAs. *Nat Rev Genet* Nov 2019; 20: 675–691.
10. Yang P, Gao R, Zhou W, et al. Protective impacts of circular RNA VMA21 on lipopolysaccharide-engendered WI-38 cells injury via mediating microRNA-142-3p. *BioFactors* May 2020; 46: 381–390.
11. Liu X, Zhao P and Ge W. Knockdown of circular RNA circZNF652 remits LPS-induced inflammatory damage by regulating miR-181a. *BioFactors* Nov 2020; 46: 1031–1040.
12. Zhao T, Zheng Y, Hao D, et al. Blood circRNAs as biomarkers for the diagnosis of community-acquired pneumonia. *J Cell Biochem* Oct 2019; 120: 16483–16494.

13. Johnson HL, Liu L, Fischer-Walker C, et al. Estimating the distribution of causes of death among children age 1-59 months in high-mortality countries with incomplete death certification. *Int J Epidemiol* Aug 2010; 39: 1103–1114.
14. Wang J, Zhao X, Wang Y, et al. circRNA-002178 act as a ceRNA to promote PDL1/PD1 expression in lung adenocarcinoma. *Cell Death Dis* Jan 16 2020; 11: 32.
15. Cheng Z, Yu C, Cui S, et al. circTP63 functions as a ceRNA to promote lung squamous cell carcinoma progression by upregulating FOXM1. *Nat Commun* Jul 19 2019; 10: 3200.
16. Yan L, Ma J, Zhu Y, et al. miR-24-3p promotes cell migration and proliferation in lung cancer by targeting SOX7. *J Cell Biochem* May 2018; 119: 3989–3998.
17. Nouws J, Wan F, Finnemore E, et al. MicroRNA miR-24-3p reduces DNA damage responses, apoptosis, and susceptibility to chronic obstructive pulmonary disease. *JCI insight* Jan 25 2021; 6: e134218.
18. Lin Y and Yang Y. MiR-24 inhibits inflammatory responses in LPS-induced acute lung injury of neonatal rats through targeting NLRP3. *Pathol Res Pract* Apr 2019; 215: 683–688.
19. Livingstone C. IGF2 And cancer. *Endocr Relat Cancer* Dec 2013; 20: R321–R339.
20. Masunaga Y, Inoue T, Yamoto K, et al. IGF2 Mutations. *J Clin Endocrinol Metab* Jan 1 2020; 105: dgz034.
21. Gao YQ, Cheng HY and Liu KF. Long non-coding RNA DANCR upregulates IGF2 expression and promotes ovarian cancer progression. *Eur Rev Med Pharmacol Sci* May 2019; 23: 3621–3626.
22. Gao T, Liu X, He B, et al. Long non-coding RNA 91H regulates IGF2 expression by interacting with IGF2BP2 and promotes tumorigenesis in colorectal cancer. *Artif Cells Nanomed Biotechnol* Dec 2020; 48: 664–671.
23. Vennin C, Spruyt N, Robin YM, et al. The long non-coding RNA 91H increases aggressive phenotype of breast cancer cells and up-regulates H19/IGF2 expression through epigenetic modifications. *Cancer Lett* Jan 28 2017; 385: 198–206.
24. Zhang J, Mao F, Zhao G, et al. Long non-coding RNA SNHG16 promotes lipopolysaccharides-induced acute pneumonia in A549 cells via targeting miR-370-3p/IGF2 axis. *Int Immunopharmacol* Jan 2020; 78: 106065.
25. Fei S, Cao L and Pan L. microRNA3941 targets IGF2 to control LPSinduced acute pneumonia in A549 cells. *Mol Med Rep* Mar 2018; 17: 4019–4026.